Coordinate Interleaved OFDM With Power Distribution Index Modulation

Ali Tugberk Dogukan, *Student Member, IEEE*, Omer Furkan Tugtekin, *Student Member, IEEE*, and Ertugrul Basar, *Senior Member, IEEE*

***Abstract*— Orthogonal frequency division multiplexing with index modulation (OFDM-IM), which transmits information bits via M-ary constellation symbols and indices of the active subcarriers, is a promising OFDM-based multicarrier transmission scheme. Recently, several new schemes have been proposed by utilizing the flexibility of the OFDM-IM to meet the diverse needs of 5G networks. Coordinate interleaved OFDM-IM (CI-OFDM-IM) that conveys the real and imaginary part of the data symbols over different subcarriers and OFDM with power distribution IM (OFDM-PIM) that transmits the data symbols over high and low power subcarriers, are two OFDM-IM based schemes with additional diversity gain and improved bit error rate (BER) performance. In this letter, we propose a novel transmission scheme named as coordinate interleaved OFDM with power distribution IM (CI-OFDM-PIM), which applies coordinate interleaving and power distribution in subcarriers to achieve a higher diversity gain. The average bit error probability (ABEP) for the CI-OFDM-PIM is derived and the superior error performance of the proposed scheme over benchmarks are shown via computer simulations.**

***Index Terms*— OFDM, index modulation, coordinate interleaving, diversity gain.**

I. Introduction

ORTHOGONAL frequency division multiplexing (OFDM) is one of the most commonly used multi-carrier transmission schemes which has been included in several communication standards thanks to its various advantages such as robustness to inter-symbol interference, simplicity and suitability. OFDM with index modulation (OFDM-IM) [1], is an OFDM-based scheme in which information bits are conveyed via not only M-ary symbols as in conventional OFDM, but also indices of the active subcarriers. In order to meet the various requirements of applications in 5G networks, such as high reliability, high data rate, low complexity, and high energy efficiency, many schemes have been proposed by utilizing the flexibility of IM. For example, sparse-encoded codebook IM (SE-CBIM) [2] and OFDM with generalized index modulation (OFDM-GIM) [3], which are OFDM-IM variants, have been proposed for ultra-reliable low-latency communications (URLLC) to enable high reliability in mission-critical applications and enhanced mobile broadband (eMBB) applications to provide high data rate transmission, respectively.

Manuscript received 20 May 2022; accepted 31 May 2022. Date of publication 2 June 2022; date of current version 12 August 2022. This study was supported by TUBITAK 2244 project under grant number 119C157 and Vestel Electronics. The associate editor coordinating the review of this letter and approving it for publication was M. Wen. *(Corresponding author: Ertugrul Basar.)*

The authors are with the Communications Research and Innovation Laboratory (CoreLab), Department of Electrical and Electronics Engineering, Koç University, Sariyer, 34450 Istanbul, Turkey (e-mail: adogukan18@ku.edu.tr; otugtekin15@ku.edu.tr; ebasar@ku.edu.tr).

Digital Object Identifier 10.1109/LCOMM.2022.3179990

Furthermore, it is challenging to provide high spectral efficiency with OFDM-IM due to its deactivated subcarriers. To overcome this disadvantage, OFDM with in-phase/quadrature index modulation (OFDM-IQ-IM) [4], has been proposed where IM is performed both in-phase and quadrature components of data symbols. Moreover, dual-mode aided OFDM-IM (DM-OFDM) [5] is proposed, where a second signal constellation is used to activate null subcarriers. Additionally, multiple distinguishable modes are obtained by partitioning the signal constellation and their permutations are exploited to convey additional bits in [6]. Nonetheless, these schemes can not provide a diversity gain. A diversity order of 2 is achieved in coordinate interleaved OFDM-IM (CI-OFDM-IM) [7] by using different active subcarriers to transmit the real and imaginary parts of the complex data symbols. Another scheme that provides a diversity order of 2 is OFDM with power distribution IM (OFDM-PIM) [8], where data symbols are conveyed through two distinct subcarriers with high and low power levels. In [9], a codebook design method is proposed to enhance the performance of OFDM-IM and obtain a diversity gain. In [10], linear constellation precoding method is applied to OFDM-IQ-IM to provide a diversity gain. Additionally, a joint selection of mode activation and subcarrier activation patterns is applied and data symbols are repetition coded over multiple subcarriers in super mode OFDM-IM (SuM-OFDM-IM) [11], resulting in higher spectral efficiency and additional diversity gain. In addition, novel transmission schemes based on multiple mode structure providing a diversity order of 2 are proposed recently in [12], [13]. A comprehensive survey and detailed literature review for OFDM-IM-based schemes can be found in [14].

In this letter, we propose a novel scheme called *coordinate interleaved OFDM with power distribution IM (CI-OFDM-PIM)*, which further enhances the diversity gain of IM-based schemes. In the proposed scheme, data symbols are first rotated and coordinate interleaved, then distributed over two different subcarriers with high and low power levels. Due to its clever subcarrier activation pattern (SAP) selection strategy, coordinate interleaving, and power distribution, the proposed method can provide a diversity gain which is equal to the subblock size. Since power distribution method makes the repeated coordinate interleaved data symbols distinguishable by multiplying them with two different power levels, transmitting information bits by IM becomes possible. Moreover, the optimum power levels and rotation angles have been obtained to maximize the minimum coding gain distance (MCGD). Transceiver architecture for the proposed scheme is given and upper bound for the average bit error probability (ABEP) is derived. It is demonstrated via computer simulations that proposed scheme has better error performance

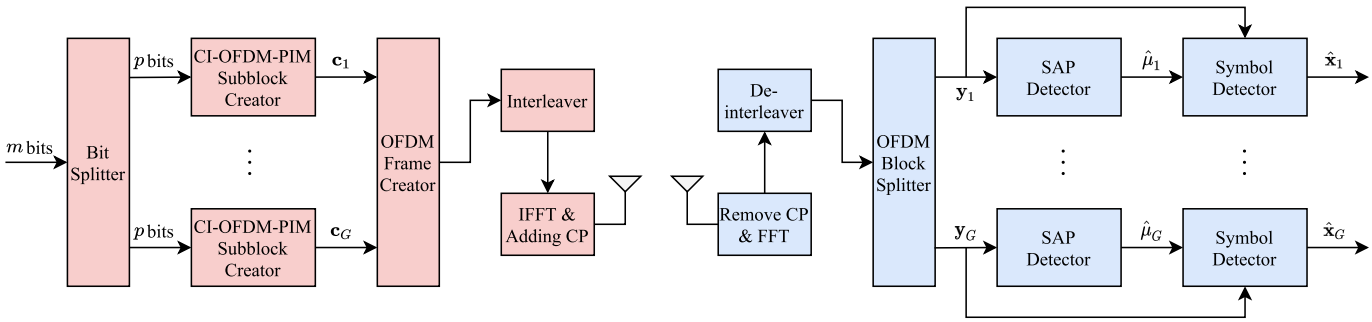

Fig. 1. Transceiver architecture of CI-OFDM-PIM including single-symbol ML detector.

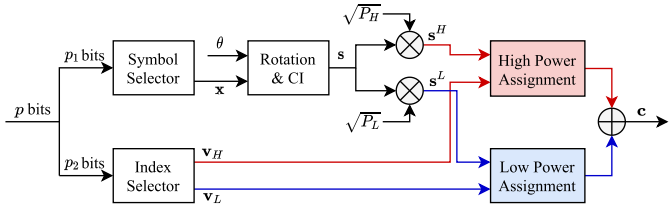

Fig. 2. The block diagram of the creation of the gth subblock of CI-OFDM-PIM.

than its benchmarks with a diversity order of 2 such as CI-OFDM-IM and OFDM-PIM due to its enhanced diversity gain.

The remainder of this letter can be summarized as follows. In Section II, the system model is proposed, in Section III, theoretical analysis for the proposed scheme is presented and the rotation angle and power level optimization is explained, and Section IV presents computer simulation results to make a comparison between the proposed scheme and its benchmarks. Finally, Section V concludes the letter.

II. System Model

CI-OFDM-PIM is based on an OFDM transmission system with S number of subcarriers as seen in Fig. 1. A total number of m bits enter the transmitter and those are separated into G blocks, where each group includes $m/G = p = p_1 + p_2$ bits, to form a subblock with length $N = S/G$, where N is an even number and greater than 2. Since the same process is applied to all subblocks, we present the creation of gth subblock $\mathbf{c}_g$, $g = [1, \cdots, G]$. For the sake of simplicity, we remove the subscript g. The block diagram for the generation of the gth subblock is given in Fig. 2. Firstly, $p_1 = (N/2)\log_2(M)$ bits determine the $N/2$ data symbols $\mathbf{x} = [x_1, \cdots, x_{N/2}]^{\mathrm{T}} \in \mathbb{C}^{N/2}$, where M and $[\cdot]^{\mathrm{T}}$ are the modulation order and transposition operation, respectively. Constellation rotation, which is a must to obtain a diversity gain and increase the coding gain, is a significant component of a coordinate interleaving-based transmission schemes [15]. The nth element of $\mathbf{x}$ is rotated with an angle θ_n, $n = 1, 2, \cdots, N/2$, and the rotated data symbol vector is obtained as:

$$\begin{aligned}\mathbf{x}^{\theta} &= [x_1 e^{j\theta_1}, x_2 e^{j\theta_2}, \cdots, x_{N/2} e^{j\theta_{N/2}}]^{\mathrm{T}} \\ &= [\bar{x}_1, \bar{x}_2, \cdots, \bar{x}_{N/2}]^{\mathrm{T}}. \end{aligned} \tag{1}$$

After this, CI is applied to $\mathbf{x}^{\theta}$ and coordinate interleaved data symbol vector is obtained as:

$$\mathbf{s} = \begin{bmatrix} s_1 \\ s_2 \\ \vdots \\ s_{N/2-1} \\ s_{N/2} \end{bmatrix} = \begin{bmatrix} \bar{x}_1^R + j\bar{x}_2^I \\ \bar{x}_2^R + j\bar{x}_1^I \\ \vdots \\ \bar{x}_{N/2-1}^R + j\bar{x}_{N/2}^I \\ \bar{x}_{N/2}^R + j\bar{x}_{N/2-1}^I \end{bmatrix}. \tag{2}$$

Here, two power levels are specified as P_H (high) and P_L (low) for the subcarriers with high and low power, respectively, where $P_H > P_L$ and $P_H + P_L = 2$ since the average power of a subcarrier is normalized to unity, i.e., $E\{\mathbf{c}^{\mathrm{H}}\mathbf{c}\} = N$, where $E\{\cdot\}$ and $(\cdot)^{\mathrm{H}}$ represents expectation and Hermitian transposition, respectively. Then, $p_2 = \log_2(N)$ bits determine the SAP $\mathbf{v} = [v_1, v_2, \cdots, v_N]^{\mathrm{T}}$, $v_\chi \in \{1, \cdots, N\}$, $\chi = 1, 2, \cdots, N$. Note that the method for creating SAPs and the reason for using only N SAPs to convey bits are given as a remark in the following. The first half and second half of $\mathbf{v}$ represent the indices of subcarriers with high power and low power as $\mathbf{v}_H = [v_1, \cdots, v_{N/2}]^{\mathrm{T}}$ and $\mathbf{v}_L = [v_{N/2+1}, \cdots, v_N]^{\mathrm{T}}$, respectively. As a result, a total number of $p = p_1 + p_2 = (N/2)\log_2(M) + \log_2(N)$ bits can be conveyed for each subblock. After that, the coordinate interleaved data symbol vector is multiplied with $\sqrt{P_H}$ and $\sqrt{P_L}$, then high and low power data symbol vectors are obtained as $\mathbf{s}^H = \sqrt{P_H}\mathbf{s}$ and $\mathbf{s}^L = \sqrt{P_L}\mathbf{s}$, respectively. Finally, the entries of $\mathbf{s}^H$ and $\mathbf{s}^L$ are placed into the target subblock $\mathbf{c}$ with the entries of $\mathbf{v}_H$ and $\mathbf{v}_L$, respectively. The selection strategy of P_H, P_L, and $\boldsymbol{\theta} = [\theta_1, \cdots, \theta_{N/2}]^{\mathrm{T}}$ is discussed in the Section III.

Remark (SAP Creation): The minimum distance of a set $\mathcal{Z}$ of codewords with length N_c is defined as $d = \min_{z_1, z_2 \in \mathcal{Z}, z_1 \neq z_2} d(z_1, z_2)$, where $d(z_1, z_2)$ represents the Hamming distance between z_1 and z_2. In a Q-ary block code of length N_c and minimum distance d, the number $A_Q(N_c, d)$ indicates the maximum number of possible codewords. Here, Singleton bound states that $A_Q(N_c, d) \leq Q^{N_c - d + 1}$ [16]. In the proposed method, all possible SAPs can be considered as codewords in a N-ary block code of length N. To provide a diversity order of N, d should be selected as N; hence, a total $Q^{N_c - d + 1} = N^{N - N + 1} = N$ number of SAPs can be utilized for the transmission of index bits according to the Singleton bound. There are a total number of $2^{p_2} = N$ possible SAPs. The first SAP is given as $(\mathbf{v})_1 = [1, 2, \cdots, N]^{\mathbf{T}}$ and

TABLE I
THE SUBCARRIER INDICES ACCORDING TO INCOMING p_2 BITS FOR $N = 4$

p_1 bits	$\mathbf{v}_H^{\mathrm{T}}$	$\mathbf{v}_L^{\mathrm{T}}$	$\mathbf{c}^{\mathrm{T}}$
[00]	[1, 2]	[3, 4]	$[s_1^H s_2^H s_1^L s_2^L]$
[01]	[4, 1]	[2, 3]	$[s_2^H s_1^L s_2^L s_1^H]$
[10]	[3, 4]	[1, 2]	$[s_1^L s_2^L s_1^H s_2^H]$
[11]	[2, 3]	[4, 1]	$[s_2^L s_1^H s_2^H s_1^L]$

μth SAP $(\mathbf{v})_\mu$ can be obtained by circularly shifting $(\mathbf{v})_1$ with $\mu - 1$ elements.

For simplicity, we provide an example below for the creation of a subblock.

Example: Assume that $N = 4$, $p_2 = [0\,0]$, $\mathbf{s} = [s_1\ s_2]^{\mathrm{T}}$, and all possible SAPs can be obtained as in Table I. There are $N = 4$ possible $\mathbf{v} = [\mathbf{v}_H^{\mathrm{T}} \mathbf{v}_L^{\mathrm{T}}]^{\mathrm{T}}$ vectors and the Hamming distance between each $\mathbf{v}$ pair is $N = 4$. According to incoming $p_2 = [0\,0]$ bits, $\mathbf{v}_H = [1, 2]^{\mathrm{T}}$ and $\mathbf{v}_L = [3, 4]^{\mathrm{T}}$. With these parameters, the example subblock is created as:

$$\mathbf{c} = [s_1^H, s_2^H, s_1^L, s_2^L]^{\mathrm{T}}, \tag{3}$$

where $s_a^H = \sqrt{P_H} s_a$ and $s_a^L = \sqrt{P_L} s_a$ represent the coordinate interleaved data symbols with high and low power, respectively, and $a = 1, 2$.

By following the same steps for all subblocks, the whole OFDM frame is generated. Then, a block-type interleaver is applied as in [7]. After taking inverse fast Fourier transform (IFFT) and inserting cyclic prefix (CP) with length S_{CP}, the time-domain signal is obtained and transmitted over T-tap frequency selective Rayleigh fading channel whose elements follow $\mathcal{CN}(0, 1/T)$ distribution. At the receiver side, after removing CP, FFT and deinterleaver are applied to obtain the frequency domain signal. The equivalent input-output equation for the gth subblock in the frequency domain can be indicated as:

$$\mathbf{y}_g = \mathbf{C}_g \mathbf{h}_g + \mathbf{w}_g, \tag{4}$$

where $\mathbf{y}_g$, $\mathbf{h}_g = [h_{g,1}, \cdots, h_{g,N}]^{\mathrm{T}}$, and $\mathbf{w}_g = [w_{g,1}, \cdots, w_{g,N}]^{\mathrm{T}}$ are the received signal vector, channel coefficients, and noise vector for the corresponding gth subblock, respectively, where $h_\epsilon \sim \mathcal{CN}(0, 1)$, $w_\epsilon \sim \mathcal{CN}(0, N_0)$, $\epsilon = 1, \cdots, N$, and $\mathbf{C}_g = \mathrm{diag}(\mathbf{c}_g)$, $\mathrm{diag}(\cdot)$ is the diagonalization. We define the signal-to-noise (SNR) ratio as $\Gamma = E_b/N_0$, where $E_b = (S + S_{\mathrm{CP}})/m$ is the average bit energy. In order to detect the gth subblock, the maximum-likelihood (ML) rule can be applied by employing the set $\{\mathbf{c}_1, \mathbf{c}_2, \cdots, \mathbf{c}_{2^p}\} \in \mathcal{C}$ which consists of all possible subblock realizations:

$$\hat{\mathbf{c}}_g = \arg \min_{\mathbf{c}_g \in \mathcal{C}} \|\mathbf{y}_g - \mathbf{C}_g \mathbf{h}_g\|^2. \tag{5}$$

The number of metrics calculated in (5) is $NM^{N/2}$ and therefore, the ML detector becomes significantly complicated for high values of N and M. The number of metrics calculated for detection can be reduced by exploiting single-symbol ML decoding property of CIODs as in [7]. For the gth subblock, (4) may be rewritten without losing generality as follows:

$$\begin{bmatrix} y_1 \\ \vdots \\ y_N \end{bmatrix} = \begin{bmatrix} c_1 & & \\ & \ddots & \\ & & c_N \end{bmatrix} \begin{bmatrix} h_1 \\ \vdots \\ h_N \end{bmatrix} + \begin{bmatrix} w_1 \\ \vdots \\ w_N \end{bmatrix}. \tag{6}$$

For each realization of $(\mathbf{v})_\mu = ([\mathbf{v}_H^{\mathrm{T}} \mathbf{v}_L^{\mathrm{T}}]^{\mathrm{T}})_\mu$, $\mu = 1, \cdots, N$, N equivalent channel models can be obtained for each pair of $(\mathbf{x}_\alpha, \mathbf{x}_\beta)$ by the ML detector as in (7), as shown at the bottom of the next page, where $\mathbf{x}_\gamma = [x_\gamma^H\ x_\gamma^L]^{\mathrm{T}}$, $\gamma \in \{\alpha, \beta\}$. We can rewrite (7) as:

$$\begin{aligned} (\tilde{\mathbf{y}}_\xi)_\mu &= (\tilde{\mathbf{H}}_\xi)_\mu \tilde{\mathbf{x}}_\xi + (\tilde{\mathbf{w}}_\xi)_\mu \\ &= [(\tilde{\mathbf{H}}_{\xi,1})_\mu\ (\tilde{\mathbf{H}}_{\xi,2})_\mu] \tilde{\mathbf{x}}_\xi + (\tilde{\mathbf{w}}_\xi)_\mu, \end{aligned} \tag{8}$$

where $\xi = 1, 2, \cdots, N/4$, $\alpha = 2\xi - 1$ and $\beta = 2\xi$. Since the columns of $(\tilde{\mathbf{H}}_\xi)_\mu$ are orthogonal, single symbol ML decoding can be applied and for each $(\mathbf{v})_\mu$ realization, the ML decoder computes the following metrics as:

$$\begin{aligned} \Delta(\mu) = \sum_{\xi=1}^{N/4} \Big(&\min_{x_\alpha} \|(\tilde{\mathbf{y}}_\xi)_\mu - (\tilde{\mathbf{H}}_{\xi,1})_\mu \tilde{\mathbf{x}}_\alpha\|^2 \\ &+ \min_{x_\beta} \|(\tilde{\mathbf{y}}_\xi)_\mu - (\tilde{\mathbf{H}}_{\xi,2})_\mu \tilde{\mathbf{x}}_\beta\|^2 \Big), \end{aligned} \tag{9}$$

where $\tilde{\mathbf{x}}_\gamma = [x_\gamma^{(H,R)}\ x_\gamma^{(H,I)}\ x_\gamma^{(L,R)}\ x_\gamma^{(L,I)}]^{\mathrm{T}}$. Here, firstly, activated SAP $(\mathbf{v})_{\hat{\mu}}$ is determined by using $\hat{\mu} = \arg\min_{\mu} \Delta(\mu)$. Then, data symbols are decoded by using the following rules:

$$\begin{aligned} \hat{x}_\alpha &= \min_{x_\alpha} \|(\tilde{\mathbf{y}}_\xi)_{\hat{\mu}} - (\tilde{\mathbf{H}}_{\xi,1})_{\hat{\mu}} \tilde{\mathbf{x}}_\alpha\|^2 \\ \hat{x}_\beta &= \min_{x_\beta} \|(\tilde{\mathbf{y}}_\xi)_{\hat{\mu}} - (\tilde{\mathbf{H}}_{\xi,2})_{\hat{\mu}} \tilde{\mathbf{x}}_\beta\|^2. \end{aligned} \tag{10}$$

$$\begin{bmatrix} y_{v_{2\alpha-1}}^R \\ y_{v_{2\alpha-1}}^I \\ y_{v_{2\alpha}}^R \\ y_{v_{2\alpha}}^I \\ y_{v_{2\beta-1}}^R \\ y_{v_{2\beta-1}}^I \\ y_{v_{2\beta}}^R \\ y_{v_{2\beta}}^I \end{bmatrix}_\mu = \begin{bmatrix} h_{v_{2\alpha-1}}^R & 0 & 0 & 0 & 0 & -h_{v_{2\alpha-1}}^I & 0 & 0 \\ h_{v_{2\alpha-1}}^I & 0 & 0 & 0 & 0 & h_{v_{2\alpha-1}}^R & 0 & 0 \\ 0 & -h_{v_{2\alpha}}^I & 0 & 0 & h_{v_{2\alpha}}^R & 0 & 0 & 0 \\ 0 & h_{v_{2\alpha}}^R & 0 & 0 & h_{v_{2\alpha}}^I & 0 & 0 & 0 \\ 0 & 0 & h_{v_{2\beta-1}}^R & 0 & 0 & 0 & 0 & -h_{v_{2\beta-1}}^I \\ 0 & 0 & h_{v_{2\beta-1}}^I & 0 & 0 & 0 & 0 & h_{v_{2\beta-1}}^R \\ 0 & 0 & 0 & -h_{v_{2\beta}}^I & 0 & 0 & h_{v_{2\beta}}^R & 0 \\ 0 & 0 & 0 & h_{v_{2\beta}}^R & 0 & 0 & h_{v_{2\beta}}^I & 0 \end{bmatrix}_\mu \times \begin{bmatrix} x_\alpha^{(H,R)} \\ x_\alpha^{(H,I)} \\ x_\alpha^{(L,R)} \\ x_\alpha^{(L,I)} \\ x_\beta^{(H,R)} \\ x_\beta^{(H,I)} \\ x_\beta^{(L,R)} \\ x_\beta^{(L,I)} \end{bmatrix} + \begin{bmatrix} w_{v_{2\alpha-1}}^R \\ w_{v_{2\alpha-1}}^I \\ w_{v_{2\alpha}}^R \\ w_{v_{2\alpha}}^I \\ w_{v_{2\beta-1}}^R \\ w_{v_{2\beta-1}}^I \\ w_{v_{2\beta}}^R \\ w_{v_{2\beta}}^I \end{bmatrix}_\mu . \tag{7}$$

The same process is performed to detect SAPs, $(\mathbf{v})_{\hat{\mu}_1}, \cdots, (\mathbf{v})_{\hat{\mu}_G}$, and data symbols, $\hat{\mathbf{x}}_1, \cdots, \hat{\mathbf{x}}_G$, of all subblocks, $\hat{\mathbf{x}} = [\hat{x}_1, \cdots, \hat{x}_{N/2}]^{\mathrm{T}}$. Thanks to single-symbol ML detection, the number of metrics calculated for decoding decreases from $NM^{N/2}$ to $(N/2)NM$.

III. Performance Analysis and Optimization

In this section, we obtain an upper bound on the BER of CI-OFDM-PIM system under the assumption of ML detection. As in [1], ABEP of CI-OFDM-PIM can be obtained as:

$$P_b = \frac{1}{p2^p} \sum_{\mathbf{C},\hat{\mathbf{C}}} \mathrm{P}(\mathbf{C} \to \hat{\mathbf{C}}) \mathrm{e}(\mathbf{C}, \hat{\mathbf{C}}), \tag{11}$$

where $\mathrm{e}(\mathbf{C}, \hat{\mathbf{C}})$ is the number of erroneous bits when $\mathbf{C}$ is transmitted; however, $\hat{\mathbf{C}}$ is incorrectly detected and $\mathrm{P}(\mathbf{C} \to \hat{\mathbf{C}})$ is the pairwise error event for the corresponding pairwise event and given by

$$\mathrm{P}(\mathbf{C} \to \hat{\mathbf{C}}) \approx \frac{1/4}{\det(\mathbf{I}_N + (\Gamma/3)\mathbf{D})} + \frac{1/12}{\det(\mathbf{I}_N + (\Gamma/4)\mathbf{D})}, \tag{12}$$

where $\mathbf{I}_N$ and $\mathbf{D} = (\mathbf{C} - \hat{\mathbf{C}})^{\mathrm{H}}(\mathbf{C} - \hat{\mathbf{C}})$ are $N \times N$ identity matrix and difference matrix, respectively.

In order to investigate the diversity order of CI-OFDM-PIM, two cases are considered: (1) detecting index bits erroneously and (2) detecting single or multiple data symbols under the condition of detecting index bits correctly. For case (1), assume that $p_2 = [00]$, $\mathbf{v} = [1, 2, 3, 4]^{\mathrm{T}}$, bits are transmitted; nonetheless, $[01]$ bits, $\hat{\mathbf{v}} = [4, 1, 2, 3]^{\mathrm{T}}$, are decoded incorrectly from Table I. As seen from this example, the Hamming distance between $\mathbf{v}$ and $\hat{\mathbf{v}}$ is $N = 4$. This result is valid for all other pairwise $(\mathbf{v}, \hat{\mathbf{v}})$ events and it can be concluded that the diversity order is always 4 for case (1). For case (2), assume that $\mathbf{c}$ with data symbols $(\bar{x}_1, \bar{x}_2)$, is transmitted, and $\hat{\mathbf{c}}$ with $(\bar{x}_1, \hat{\bar{x}}_2)$, is decoded erroneously with a single symbol error $(\bar{x}_2 \to \hat{\bar{x}}_2)$. This pair $(\mathbf{c}, \hat{\mathbf{c}})$ is given as:

$$\begin{aligned} \mathbf{c} &= [(\bar{x}_1^R + j\bar{x}_2^I)^H, (\bar{x}_2^R + j\bar{x}_1^I)^H, (\bar{x}_1^R + j\bar{x}_2^I)^L, \\ &\quad (\bar{x}_2^R + j\bar{x}_1^I)^L]^{\mathrm{T}} \\ \hat{\mathbf{c}} &= [(\bar{x}_1^R + j\hat{\bar{x}}_2^I)^H, (\hat{\bar{x}}_2^R + j\bar{x}_1^I)^H, (\bar{x}_1^R + j\hat{\bar{x}}_2^I)^L, \\ &\quad (\hat{\bar{x}}_2^R + j\bar{x}_1^I)^L]^{\mathrm{T}}. \end{aligned} \tag{13}$$

As seen from (13), only one symbol error causes changes over all subcarriers that resulting a diversity order of $r = N = 4$, where $r = \mathrm{rank}(\mathbf{D})$. Consequently, when non-zero and different rotation angles $[\theta_1, \cdots, \theta_{N/2}]$ are selected, we provide $\min_{\mathbf{C},\hat{\mathbf{C}}}(r) = 4$ which demonstrates that the diversity order of the proposed system is 4. By induction, the extension of cases (1) and (2) is valid for any value of N; hence, a diversity order of N is always provided.

The rotation angles $\boldsymbol{\theta}$ and power levels (P_H, P_L) affect the non-zero eigenvalues of $\mathbf{D}$ being λ_ζ, $\zeta = 1, 2, \cdots, N$, and as a consequence the ABEP. For simplicity, we define a single power level P, $0 < P < 1$, and rotation angle θ, where $P_H = 2 - P$, $P_L = P$, and θ_n is calculated with respect to θ as discussed in the sequel for $n = 1, \cdots, N/2$. We consider the worst case pairwise error probability (PEP) events to obtain the optimum θ and P values as:

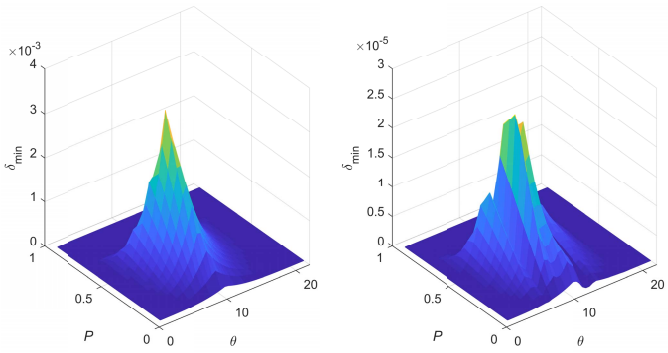

Fig. 3. MCGD variation with respect to P and θ for 4-QAM and 8-QAM constellations, respectively.

$$(\theta_{\mathrm{opt}}, P_{\mathrm{opt}}) = \arg \max_{\theta,P} \delta_{\min}. \tag{14}$$

Here, $\delta_{\min} = \min_{\mathbf{C},\hat{\mathbf{C}}} \prod_{\zeta=1}^{N} \lambda_\zeta$ is the MCGD, which is a significant parameter for the minimization of (12). Due to a joint search over all possible P and θ_n values is not practically feasible, we propose a heuristic and near-optimal solution to find θ_{opt} and P_{opt} as follows. Since quadrature amplitude modulation (QAM) constellation repeats itself every $90°$, we divide $90°$ into $N/2$ parts. In this case, we define the nth rotation angle as $\theta_n = \theta + 180(n-1)/N$, $0 < \theta < 90/N$, $n = 1, \cdots, N/2$. For example, as seen from Fig. 3, $(\theta_{\mathrm{opt}}, P_{\mathrm{opt}})$ can be obtained by exhaustive search as $(8.5°, 0.45)$ and $(8°, 0.40)$ for 4-QAM and 8-QAM, respectively, when $N = 4$. Here, the step sizes for $(\theta_{\mathrm{opt}}, P_{\mathrm{opt}})$ are $(0.5, 0.05)$. For higher values of M and N, carrying out an exhaustive search over all possible $(\mathbf{C}, \hat{\mathbf{C}})$ pairs is not practical. In this case, δ_{min} is evaluated for $\mathbf{C} \in \{\mathbf{C}^1\}$ and $\hat{\mathbf{C}} \in \{\mathbf{C}^1, \mathbf{C}^2\}$, where $\mathbf{C}^1 = \mathrm{diag}([s_1^H, s_2^H, s_1^L, s_2^L]^{\mathrm{T}})$ and $\mathbf{C}^2 = \mathrm{diag}([s_1^L, s_2^L, s_1^H, s_2^H]^{\mathrm{T}})$ are baseline worst case error events for $N = 4$. Here, two PEP events are considered: $i)$ $(\mathbf{C}^1 \to \mathbf{C}^1)$: correct SAP with single erroneous data symbol, $ii)$ $(\mathbf{C}^1 \to \mathbf{C}^2)$: detecting SAP as $N/2$ circularly shifted version of it with correct or erroneous data symbols.

IV. Simulation Results and Comparisons

In this section, simulation results are demonstrated to compare CI-OFDM-PIM with benchmark schemes, given that the system parameters are $S = 128$, $S_{CP} = 16$ and $T = 10$ tap Rayleigh fading channel whose elements are independent identically distributed (i.i.d.) complex Gaussian distributed random variables. For convenience, we will refer to "OFDM-IM (N, v)" as OFDM-IM scheme with v out of N subcarriers are active, "DM-OFDM (N, v)" as DM-OFDM scheme where v out of N subcarriers exploits the primary M-ary PSK(or QAM) constellations, "SuM-OFDM-IM (M, Q)" as SuM-OFDM-IM scheme with Q symbols included in each M mode, "CI-OFDM-IM (N, v)" as CI-OFDM-IM scheme with v out of N subcarriers are active, "OFDM-PIM (N, P)" as OFDM-PIM scheme with N subcarriers and optimum power of P, "RC-OFDM (n)" as RC-OFDM scheme with a

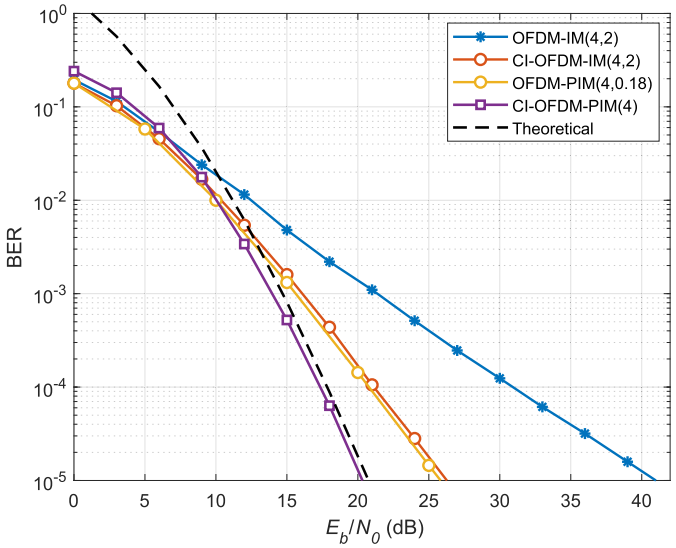

Fig. 4. Error performance comparison of CI-OFDM-PIM with benchmark schemes when $N = 4$ and $M = 4$ for a spectral efficiency of 1.5 bps/Hz.

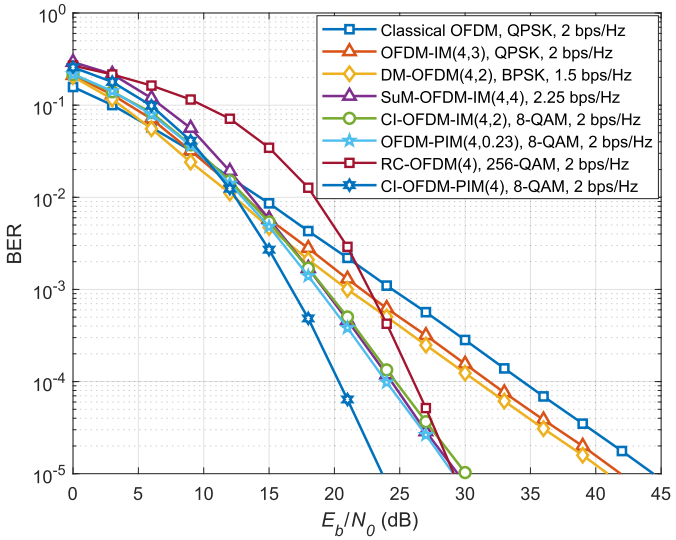

Fig. 5. Error performance comparison of CI-OFDM-PIM with benchmark schemes.

repetition rate of n and "CI-OFDM-PIM (N)" is the proposed CI-OFDM-PIM scheme with N subblock length. Optimum angle and power level for the CI-OFDM-PIM is determined based on the selection strategy discussed in the Section III.

As seen in the Fig. 4, theoretical BER curve, which is obtained by (11), acts as an upper bound for CI-OFDM-PIM. Furthermore, CI-OFDM-PIM provides approximately 6 dB gain over CI-OFDM-IM and OFDM-PIM due to its higher diversity gain at a BER value of 10^{-5} when $N = 4$, $M = 4$, and the spectral efficiency is 1.5 bps/Hz.

In Fig. 5, the error performance of CI-OFDM-PIM is compared with classical OFDM, OFDM-IM, DM-OFDM, SuM-OFDM-IM, CI-OFDM-IM, OFDM-PIM, and RC-OFDM by using the ML detector. As seen from Fig. 5, CI-OFDM-PIM outperforms the other schemes in terms of error performance. At a BER value of 10^{-5}, CI-OFDM-PIM achieves approximately 6 dB gain over the closest rivals, which are CI-OFDM-IM, OFDM-PIM, RC-OFDM, and SuM-OFDM-IM. Moreover, the error performance gap between CI-OFDM-PIM and the schemes with diversity order of 2 further extends as the SNR value increases thanks to its higher BER vs SNR slope caused by diversity order of 4.

V. Conclusion

In this letter, we have proposed a novel OFDM-IM based transmission scheme called CI-OFDM-PIM. CI-OFDM-PIM provides remarkable error performance by benefiting from CI and power distribution. CI-OFDM-PIM outperforms its benchmarks with a diversity order of 2 such as CI-OFDM-IM, OFDM-PIM and RC-OFDM by 6 dB gain due to its superior diversity gain which is equal to the number of subcarriers in each subblock. CI-OFDM-PIM can have a great potential for next generation wireless networks thanks to its advantages such as outstanding BER performance and high diversity gain. The generalization of CI-OFDM-PIM for varying number of data symbols and investigation of achievable rate performance are left for our future studies.

References

[1] E. Başar, U. Aygölü, E. Panayırcı, and H. V. Poor, "Orthogonal frequency division multiplexing with index modulation," *IEEE Trans. Signal Process.*, vol. 61, no. 22, pp. 5536–5549, Nov. 2013.
[2] E. Arslan, A. T. Dogukan, and E. Basar, "Sparse-encoded codebook index modulation," *IEEE Trans. Veh. Technol.*, vol. 69, no. 8, pp. 9126–9130, Aug. 2020.
[3] R. Fan, Y. J. Yu, and Y. L. Guan, "Generalization of orthogonal frequency division multiplexing with index modulation," *IEEE Trans. Wireless Commun.*, vol. 14, no. 10, pp. 5350–5359, Oct. 2015.
[4] B. Zheng, F. Chen, M. Wen, F. Ji, H. Yu, and Y. Liu, "Low-complexity ML detector and performance analysis for OFDM with in-phase/quadrature index modulation," *IEEE Commun. Lett.*, vol. 19, no. 11, pp. 1893–1896, Nov. 2015.
[5] T. Mao, Z. Wang, Q. Wang, S. Chen, and L. Hanzo, "Dual-mode index modulation aided OFDM," *IEEE Access*, vol. 5, pp. 50–60, 2016.
[6] M. Wen, E. Basar, Q. Li, B. Zheng, and M. Zhang, "Multiple-mode orthogonal frequency division multiplexing with index modulation," *IEEE Trans. Commun.*, vol. 65, no. 9, pp. 3892–3906, Sep. 2017.
[7] E. Başar, "OFDM with index modulation using coordinate interleaving," *IEEE Wireless Commun. Lett.*, vol. 4, no. 4, pp. 381–384, Aug. 2015.
[8] A. T. Dogukan and E. Basar, "Orthogonal frequency division multiplexing with power distribution index modulation," *Electron. Lett.*, vol. 56, no. 21, pp. 1156–1159, Oct. 2020.
[9] S. Dang, G. Chen, and J. P. Coon, "Lexicographic codebook design for OFDM with index modulation," *IEEE Trans. Wireless Commun.*, vol. 17, no. 12, pp. 8373–8387, Dec. 2018.
[10] M. Wen, B. Ye, E. Basar, Q. Li, and F. Ji, "Enhanced orthogonal frequency division multiplexing with index modulation," *IEEE Trans. Wireless Commun.*, vol. 16, no. 7, pp. 4786–4801, Jul. 2017.
[11] A. T. Dogukan and E. Basar, "Super-mode OFDM with index modulation," *IEEE Trans. Wireless Commun.*, vol. 19, no. 11, pp. 7353–7362, Nov. 2020.
[12] Q. Li, M. Wen, E. Basar, H. V. Poor, B. Zheng, and F. Chen, "Diversity enhancing multiple-mode OFDM with index modulation," *IEEE Trans. Commun.*, vol. 66, no. 8, pp. 3653–3666, Aug. 2018.
[13] F. Yarkin and J. P. Coon, "Q-ary multi-mode OFDM with index modulation," *IEEE Wireless Commun. Lett.*, vol. 9, no. 7, pp. 1110–1114, Jul. 2020.
[14] T. Mao, Q. Wang, Z. Wang, and S. Chen, "Novel index modulation techniques: A survey," *IEEE Commun. Surveys Tuts.*, vol. 21, no. 1, pp. 315–348, 1st Quart., 2018.
[15] M. Z. A. Khan and B. S. Rajan, "Single-symbol maximum likelihood decodable linear STBCs," *IEEE Trans. Inf. Theory*, vol. 52, no. 5, pp. 2062–2091, May 2006.
[16] R. C. R. C. Singleton, "Maximum distance q-nary codes," *IEEE Trans. Inf. Theory*, vol. IT-10, no. 2, pp. 116–118, Apr. 1964.